AIAA SciTech Forum
9 - 13 January 2017, Grapevine, Texas
55th AIAA Aerospace Sciences Meeting

Investigation of Isolated and Installed Three-Stream Jets from Offset Nozzles

Vincent Phong* and Dimitri Papamoschou†
University of California, Irvine, Irvine, CA, 92697

An experimental aeroacoustic investigation of three-stream nozzle concepts with potential to reduce takeoff noise from future supersonic aircraft is presented. We use guidance from previous three-stream nozzle experiments to explore asymmetric designs where both secondary and tertiary streams are concentrated in the downward direction. The impact of increasing the plug size on noise is examined. Enlarging the plug provides moderate noise reduction for axisymmetric and asymmetric nozzle configurations. Nozzle configurations that combine asymmetry in both secondary and tertiary streams provide a distinct noise benefit in the sideline azimuthal direction. Considering the sound pressure level at a full-scale frequency around 300 Hz, the combined effects of the enlarged plug and dual asymmetry yield reductions of 15 dB and 6 dB in the downward and sideline azimuthal directions, respectively, and at angles close to the angle of peak emission. Installation effects with an aft deck indicate minimal impacts on radiated noise, except in the case of a long deck at a scrubbing position. In that case, the ability of the asymmetric nozzles to reduce noise is disrupted. Marginal shielding at high frequency is noted at forward observer angles.

I. Introduction

Supersonic passenger transport has not seen commercial service since the Concorde ceased operation in 2003. The prospect of commercially viable supersonic transportation hinges on enabling technologies that must demonstrate both economic efficiency and environmental acceptability. Sonic boom, fuel efficiency, airport community noise and high altitude emissions are among the many challenges that prohibit supersonic transports from re-entering service[1]. The International Civil Aviation Organization (ICAO) is enforcing stricter noise regulations (Chapter 4 minus 7 EPNdB, effective December 2017)[2], requiring innovative airframe configurations and propulsive systems that are both efficient and quiet. A viable engine for supersonic aircraft that meets these criteria may have a variable cycle, where the bypass ratio could be increased to reduce turbulent mixing noise at takeoff, and decreased during supersonic cruise to preserve engine performance[3]. Variable cycle engine technology will be enabled by two- or three- stream nozzle architectures, which would allow implementing noise reduction techniques that utilize the bypass stream.

Supersonic jet noise comprises three components: turbulent mixing noise, broadband shock-associated noise, and screech tones[4]. Experimental evidence has shown that Mach wave radiation dominates the turbulent mixing noise component of supersonic jets[5-11]. Mach waves are produced when turbulent eddies in the jet mixing layer convect at supersonic speeds with respect to the surrounding fluid. The addition of a lower speed, secondary (coannular) flow can significantly reduce Mach wave radiation under the conditions that 1) the primary eddies are subsonic with respect to the secondary stream, 2) the height of the secondary stream is large enough to allow room for disturbances from the primary eddies to decay subsonically and 3) the secondary potential core envelops the Mach wave emitting region of the primary jet[11,12].

Despite variable cycle technology, supersonic engine designs are limited to low-to-medium bypass ratios. The secondary core ends upstream of the primary potential core for externally mixed, low bypass

* Assistant Specialist, Department of Mechanical and Aerospace Engineering, vphong@uci.edu, AIAA Member
† Professor, Department of Mechanical and Aerospace Engineering, dpapamos@uci.edu, AIAA Fellow

ratio nozzle configurations. Noise reduction is marginal if the secondary core does not sufficiently envelop the primary shear layer[7]. The secondary nozzle can be tailored to induce asymmetry in the plume, at azimuthal directions where noise reduction is desired. Inducing asymmetry in the plume entails either geometrically offsetting the nozzle ducts[3,13,14], or installing devices that deflect the bypass stream[13,15,16,17]. The misalignment between the primary and secondary streams produces a thick, low-speed layer, that is oriented typically at downward and sideline azimuthal directions. The enlarged secondary core reduces the convective Mach number of the primary eddies that radiate sound in the directions of the thickened coannular flow[14]. The addition of a third (tertiary) stream opens a parameter space to explore noise reduction technologies using the aforementioned methods[13-17].

The flow field and acoustics of three-stream jets have been the focus of several investigations within the last few years. Henderson surveyed the acoustics of a three-stream configuration where the core and bypass streams are internally mixed upstream of the tertiary exit. The experiments covered a broad range of flow conditions[18]. The added tertiary flow reduced high-frequency noise at broadside and peak jet noise angles. Henderson *et al.* conducted acoustic experiments and flow field simulations of three-stream, externally-mixed, convergent nozzles[19]. Their investigation encompassed both axisymmetric and offset configurations for the tertiary stream. The offset, tertiary stream reduced noise along the thick side of the jet when the core flow is operating at supersonic conditions. Huff *et al.* assessed the capability of three-stream, offset duct configurations to meet Chapter 14 noise regulations[3]. Their results indicated that offsetting the tertiary duct alone would not reduce noise levels below sufficient margin to Chapter 14 (Chapter 4 minus 10 EPNdB). They proposed an alternative takeoff procedure to help attain this margin, however, the safety of the procedure has not yet been verified by the Federal Aviation Administration. Henderson and Wernet investigated the mean flow field and turbulence characteristics of externally mixed, convergent three-stream nozzles using stereo particle image velocimetry (PIV)[20]. Papamoschou *et al.* investigated noise reduction concepts for low bypass ratio nozzles that induced asymmetry in both secondary and tertiary streams[21]. Recently, Papamoschou *et al.* explored asymmetric design concepts for externally-mixed, externally-plugged, three-stream convergent nozzles[22]. A combination of a wedge-type deflector with duct asymmetry in the tertiary stream significantly reduced downward noise. However, only small reductions in the sideline azimuthal direction were obtained.

This study presents further developments made from previous, three-stream nozzle concepts designed by Papamoschou *et al.*[22]. We focus on experimental acoustic results for both isolated and installed nozzle configurations. For the isolated nozzle, the impact of enlarging the plug and the combined effect of asymmetry in the secondary and tertiary streams are studied. Installation effects are examined, using an aft deck modeled from a Lockheed Martin low-boom concept vehicle[23]. The extent of shielding and jet noise interaction are assessed by varying the nozzle position relative to the aft deck trailing edge. The feasibility of asymmetric nozzles to reduce noise for installed configurations is discussed.

II. Experimental Approach

A. Detailed nozzle designs

The nozzle designs in this study were based on three-stream nozzle systems being developed and tested at the NASA John H. Glenn Research Center (GRC)[20]. All designs comprised externally-mixed, externally-plugged convergent nozzles as illustrated in Figs. 1 and 2. The nozzles were reduced in scale to ensure compatibility with the flow rate capacity of the UC Irvine Jet Aeroacoustics Facility. The sub-millimeter tolerance requirements near the nozzle exit motivated a design where all nozzle components are built in one piece, using high-definition stereolithography. This manufacturing process limited the nozzle lip thickness to 0.2 mm. The material used was Accura 60 plastic (3D Systems) with tensile strength in the range of 58-68 MPa. The design comprised a fixed base on which replaceable nozzle attachments were mounted. The total pressure of each stream was measured through thin channels, of 0.75 mm diameter, integrated within the support struts of the nozzle. The channels begin at the outer surface of the attachment, followed an L-shaped path through the struts, and terminated into upstream facing ports in their respective ducts (Fig. 1).

Previous three-stream nozzle concepts developed by Papamoschou *et al.*[22] provided the framework for the nozzles designed in this study. The nozzles designed and tested in this study preserve the short-cowl modification from their work[22]. Figures 3(a) and 3(b) illustrate how the change from long- to short-cowl design shifts the secondary and tertiary duct exit planes downstream towards the primary duct exit plane. The shift downstream requires smaller secondary and tertiary exit diameters to preserve the secondary- and tertiary-to-primary exit area ratios. The reduction in nozzle size implies abrupt changes in nacelle diameter, adversely affecting the aircraft's sonic-boom signature.

Preserving the acoustic benefits of the short-cowl design with minimal impact to sonic-boom compatibility required constraining the nacelle boat-tail to the long-cowl design, nozzle AXI01U[22]. The nacelle boat-tail, illustrated qualitatively in Fig. 4, is proportional to the difference between the tertiary exit diameter and maximum nacelle diameter. The shift from the long-cowl design, Fig. 4(a), to the short-cowl design, Fig. 4(b), implies an increase in nacelle boat tail. This is conceptualized by the decrease in duct exit radius, or $\Delta r_{\mathrm{AXI01U}} > \Delta r_{\mathrm{AXI03U}}$. The short-cowl design and nacelle boat tail were simultaneously preserved by enlarging the plug until the tertiary diameter matched the baseline design, or $\Delta r_{\mathrm{AXI01U}} = \Delta r_{\mathrm{AXI04U}}$, as shown in Fig. 4(c). The enlarged-plug design, denoted AXI04U, marked the point of departure for asymmetric designs in this investigation.

Figures 3(b) and 3(c) detail the coordinates for axisymmetric nozzles tested in this study: AXI03U and AXI04U. The cross-sectional areas of all streams were ensured to be strictly convergent. Asymmetric nozzle configurations were designed to induce flow asymmetry by using one or more of the following methods: displacing the axisymmetric profiles of the secondary and/or tertiary ducts in the radial direction; integrating a wedge-type deflector in the fan stream; integrating a pair of vane-type deflectors in the fan stream. Nozzle configurations that displaced the initially axisymmetric duct profiles to induce flow asymmetry were ensured to maintain area convergence in the streamwise direction.

Figure 5 details the nozzle exit design specifications for the nominal and enlarged plug configurations tested in this study. D_3 is the exit diameter of the tertiary duct; $D_{1,\mathrm{eff}}$ is the area-based exit diameter of the primary duct; t is the width of the annulus of the secondary or tertiary nozzles; and ϕ is the azimuthal angle with respect to the downward vertical. Each subfigure displays views of the nozzles, characteristic dimensions, exit area ratios, and the normalized annulus thickness distribution, $t/D_{1,\mathrm{eff}}$, versus azimuthal angle, ϕ, at the exit of both secondary and tertiary ducts. All nozzles were designed with the same primary duct having $D_{1,\mathrm{eff}} = 13.33$ mm. The secondary-to-primary area ratio, A_2/A_1, and tertiary-to-primary area ratio, A_3/A_1, are common between all nozzles tested in this work. Configurations that incorporate a wedge-type deflector include the wedge side length, L, and half angle, δ. Reynolds Averaged Navier-Stokes (RANS) computations of the internal flow provided thrust loss estimates associated with the enlarged plug and asymmetric designs, which are included in Fig. 5.

Nozzle AXI03U is an axisymmetric, short-cowl arrangement with nominal plug size (Fig. 5(a)). Nozzle ECC08U is the quietest asymmetric nozzle tested in Ref. 22, which included asymmetry and a wedge-type deflector in the tertiary duct. The thrust loss for nozzle ECC08U is relative to AXI03U (Fig 5(c)). Nozzle AXI04U is a short-cowl design with an enlarged plug that satisfies the aforementioned boat-tail constraint (Fig. 4(c)). Nozzle AXI04U is the axisymmetric nozzle from which further asymmetric designs are explored in this work. Nozzle ECC09U features the same asymmetry and wedge deflector parameters as ECC08U, but with an enlarged plug. Nozzle ECC13U is identical to ECC09U but with a pair of vanes installed in the secondary duct. The vane cross sections are NACA 0012 shaped, with chord length $c = 4$ mm and angle of attack $\alpha = 10^{\mathrm{o}}$. The vane trailing edges were located 2 mm upstream from the secondary duct exit plane, at azimuthal locations $\phi = \pm 120^{\mathrm{o}}$. Nozzle ECC12U includes a wedge-type deflector in the tertiary stream, with annulus asymmetry in both secondary and tertiary ducts. The secondary stream asymmetry was induced by a similar exit annulus thickness distribution as the tertiary stream (Fig. 5(e)). The thrust loss for nozzles ECC09U and ECC12U are relative to AXI04U (Figs. 5(d) and 5(e)). The nozzle lip at $\phi = 180^{\mathrm{o}}$ is recessed for all asymmetric designs to avoid very thin long ducts and thus mitigate the associated viscous losses.

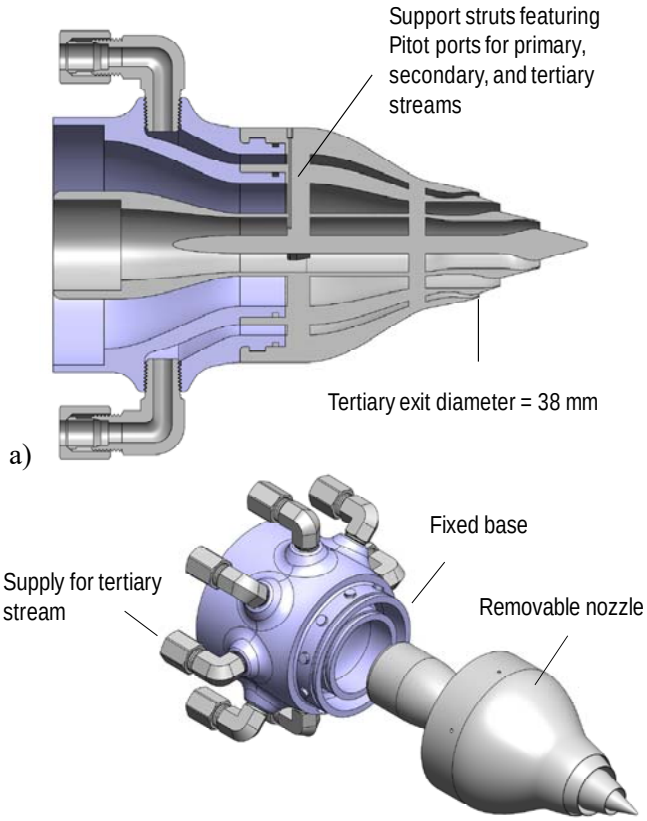

Fig. 1 CAD views of three-stream nozzle assembly. a) Cross-sectional view and b) exploded view of three-stream nozzle.

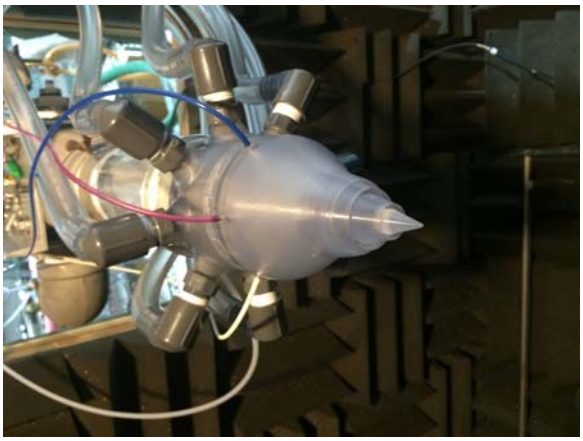

Fig. 2 Picture of three-stream nozzle assembly.

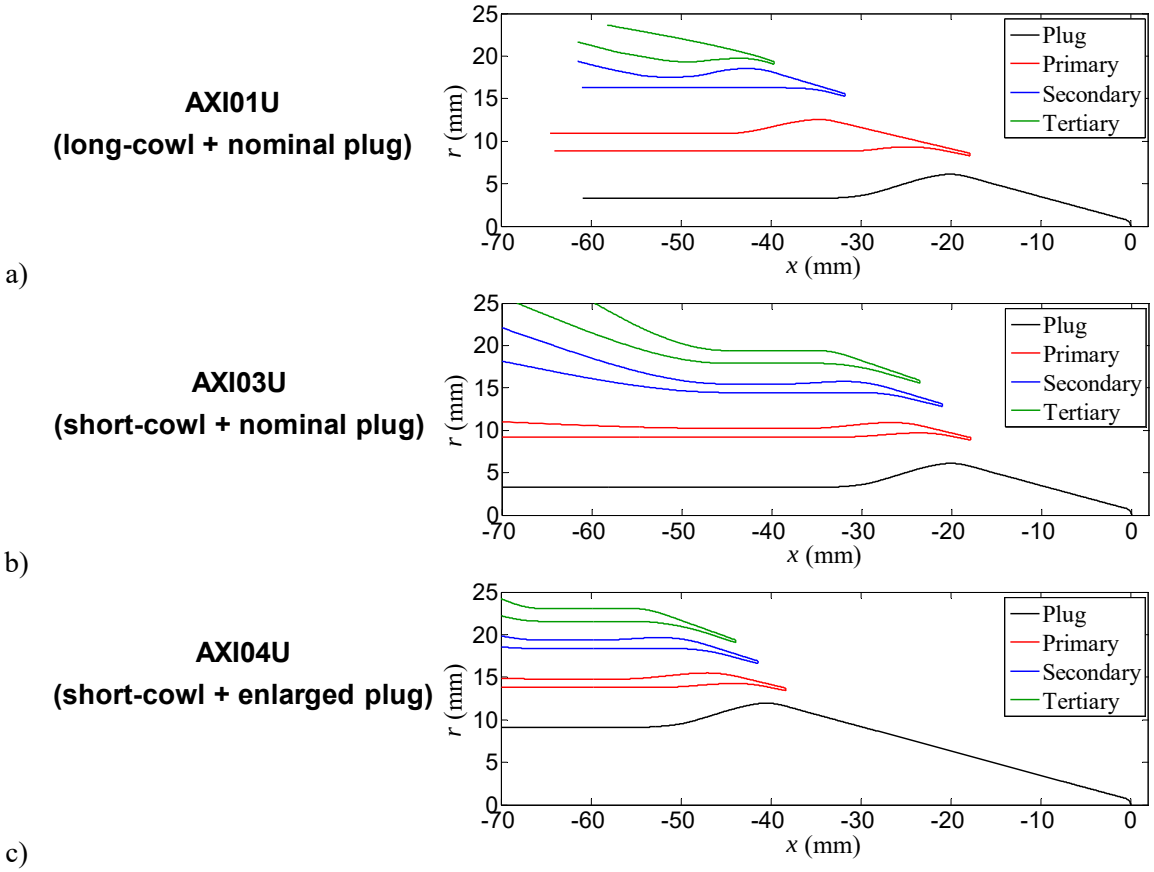

Fig. 3 Coordinates of axisymmetric nozzle configurations. a) Long-cowl with nominal plug size (AXI01U); b) short-cowl with nominal plug size (AXI02U); c) short-cowl with enlarged plug (AXI04U).

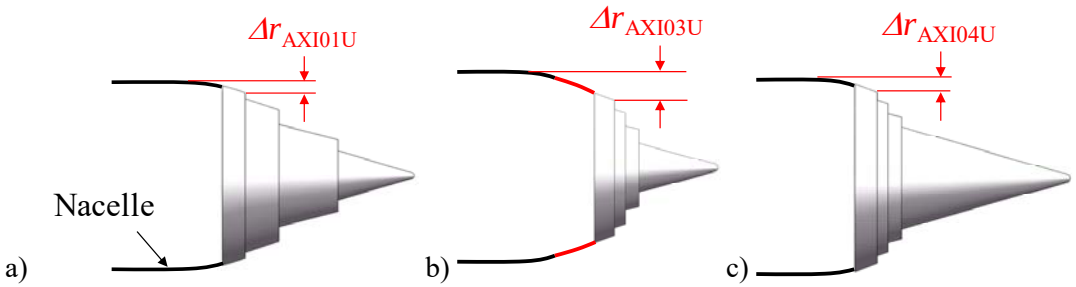

Fig. 4 Qualitative representation of nacelle boat-tail for a) long-cowl nozzle with nominal plug size (AXI01U); b) short-cowl nozzle with nominal plug size (AXI03U); c) short-cowl with enlarged plug (AXI04U).

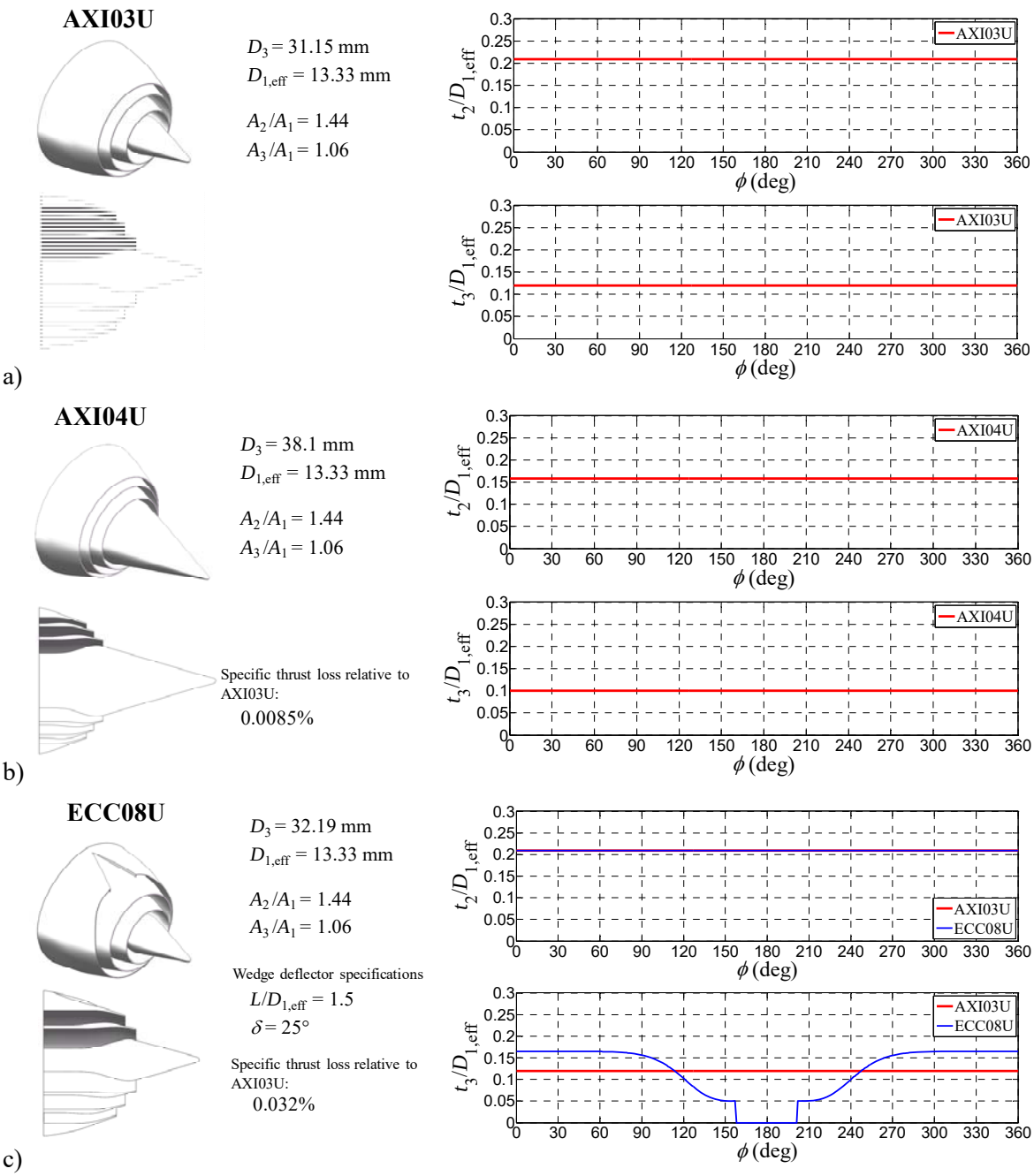

Fig 5. Nozzle exit design specifications. a) AXI03U; b) AXI04U; c) ECC08U; d) ECC09U; e) ECC12U; f) ECC13U. *Continued on next page*.

d)

ECC09U

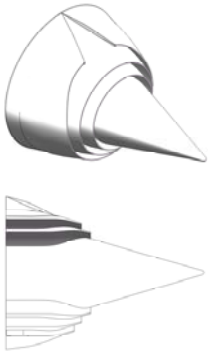

$D_3 = 39.12$ mm
$D_{1,\text{eff}} = 13.33$ mm

$A_2/A_1 = 1.44$
$A_3/A_1 = 1.06$

Wedge deflector specifications
$L/D_{1,\text{eff}} = 2.1$
$\delta = 25°$

Specific thrust loss relative to AXI04U:
0.039%

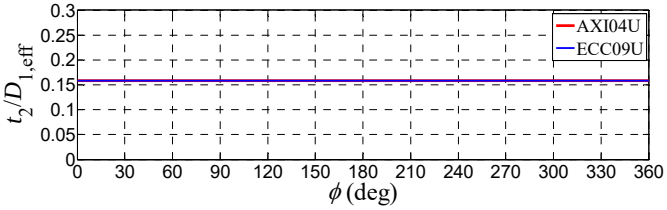

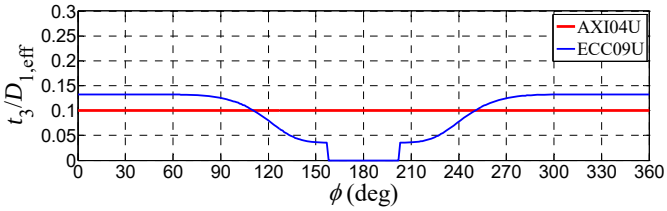

e)

ECC12U

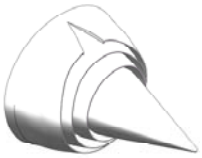

$D_3 = 40.64$ mm
$D_{1,\text{eff}} = 13.33$ mm

$A_2/A_1 = 1.44$
$A_3/A_1 = 1.06$

Wedge deflector specifications
$L/D_{1,\text{eff}} = 2.1$
$\delta = 18°$

Specific thrust loss relative to AXI04U:
0.207%

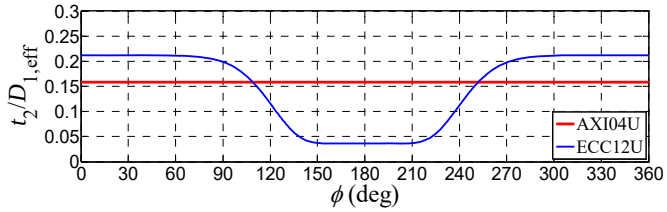

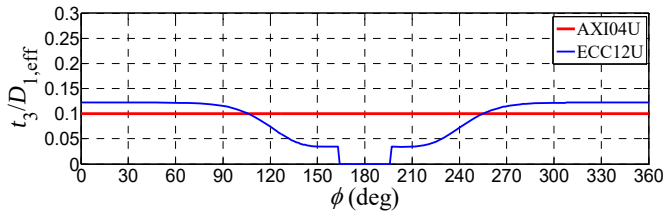

f)

ECC13U

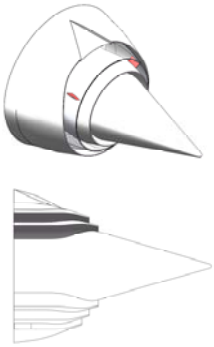

$D_3 = 40.64$ mm
$D_{1,\text{eff}} = 13.33$ mm

$A_2/A_1 = 1.44$
$A_3/A_1 = 1.06$

Wedge deflector specifications
$L/D_{1,\text{eff}} = 2.1$
$\delta = 25°$

Vane specifications
NACA 0012
$c = 4$ mm
$\alpha = 10°$

Specific thrust loss not available

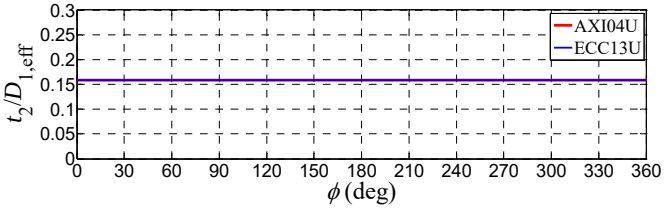

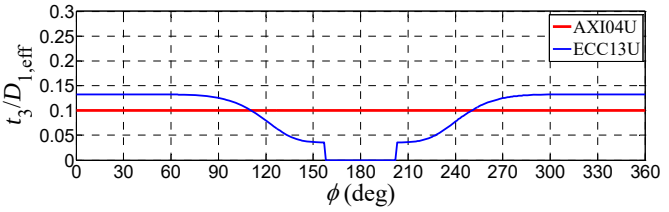

Fig 5. *Continued.*

B. Exhaust conditions

The nozzles were tested at a set point provided by NASA GRC personnel. The velocity and Mach number of each stream were matched exactly using helium-air mixture, which have been proven to simulate accurately the acoustics and fluid mechanics of hot jets[24]. Table I summarizes the exhaust conditions for each stream as tested in our facility. The nozzle pressure ratio (NPR) is the ratio of the jet stagnation pressure to ambient pressure; the nozzle temperature ratio (NTR) is the ratio of the effective (density based) jet stagnation temperature to ambient temperature; and the bypass ratio (BPR) is the ratio of either secondary or tertiary stream mass flow rate to the primary stream mass flow rate. Subscripts 1, 2

and 3 indicate the primary, secondary and tertiary streams, respectively. The total BPR for all experiments was 3.6. The Reynolds number of the primary jet was 2.6×10^5.

Table I. Cycle condition for isolated and shielded tests.

Primary			Secondary					Tertiary				
NPR_1	NTR_1	U_1, m/s	BPR_2	NPR_2	NTR_2	U_2/U_1	A_2/A_1	BPR_3	NPR_3	NTR_3	U_3/U_1	A_3/A_1
2.02	3.38	590	2.33	2.02	1.34	0.63	1.44	1.31	1.53	1.24	0.48	1.06

C. Aft deck

The airframe used for shielded acoustic tests was modeled from the Lockheed Martin N+2 low-boom configuration 1044[23]. Figure 6 depicts a rendition of the concept aircraft at two separate views. A tri-jet propulsion system is envisioned, where one engine is mounted above the aft deck center and the remaining engines suspended, on outboard pylons, below the wing. Our experiments focused solely on jet noise shielding from the top-mounted engine.

The characteristic dimensions of the aft deck assembly were provided by NASA GRC personnel. The assembled aft deck includes the aft deck trailing edge surface and canted verticals. The verticals were attached to the aft deck trailing edge surface by outboard pylons. The nozzle centerline was located on the symmetry plane of the aft deck. Figure 7 shows the NASA computer-aided design (CAD) model, UCI CAD model, and setup of the assembled aft deck in the UCI anechoic chamber. The UCI-scale aft deck and verticals were machined from 3.2-mm thick aluminum sheet metal. The aft deck trailing edge comprised two plates, hinged at the center to emulate the dihedral of the full scale aft deck trailing edge. The aft deck leading edge surfaces were notched near the center to permit experiments with the aft deck installed at the nozzle lipline (Figs. 7(b) and 7(c)).

The jet noise shielding experiments comprised parametric variations of the aft deck axial and radial positions. The positioning was aided by RANS computations of the mean velocity field of the isolated jet[22], from which the edge of the jet was defined as the radial location where the mean axial velocity equals 30 m/s. This assessment did not consider changes to the mean flow caused by the proximity of the aft deck. The aft deck radial and axial positions were defined relative to the nozzle plug tip and tertiary exit plane, respectively, as illustrated in Fig. 8. X_{TE} is the axial distance from the tertiary duct exit plane to the aft deck trailing edge; D_3 is the geometric exit diameter of the tertiary nozzle; Z is the minimum radial distance from the plug tip to the aft deck surface; and g is the gap between the jet edge and the aft deck trailing edge. Table II lists the nozzles and aft deck positions tested in this study. Two aft deck lengths were tested: X_{TE}/D_3=2.2 (nominal) and 3.7 (elongated). For each aft deck length, two radial positions were tested: the lipline position, $Z=D_3/2$, and a radial position where the estimated gap between the aft deck trailing edge and the jet edge is $g=0.1\times D_{eq}$. D_{eq}=25.0 mm is the equivalent diameter based on the total exit area of the nozzle.

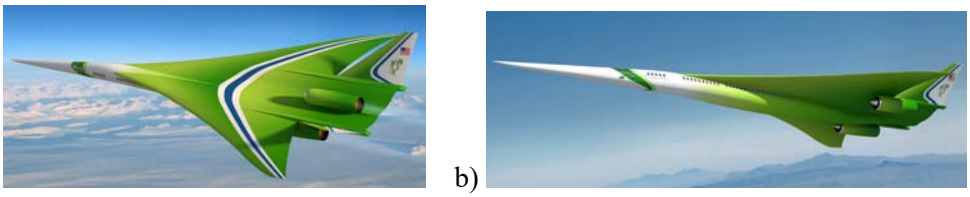

a) b)

Fig. 6 Lockheed Martin N+2 low-boom vehicle configuration 1044[23]. Views of a) engine mounted on top, center of aft deck; b) engines mounted outboard, below the wing.
Image credit: NASA/Lockheed Martin.

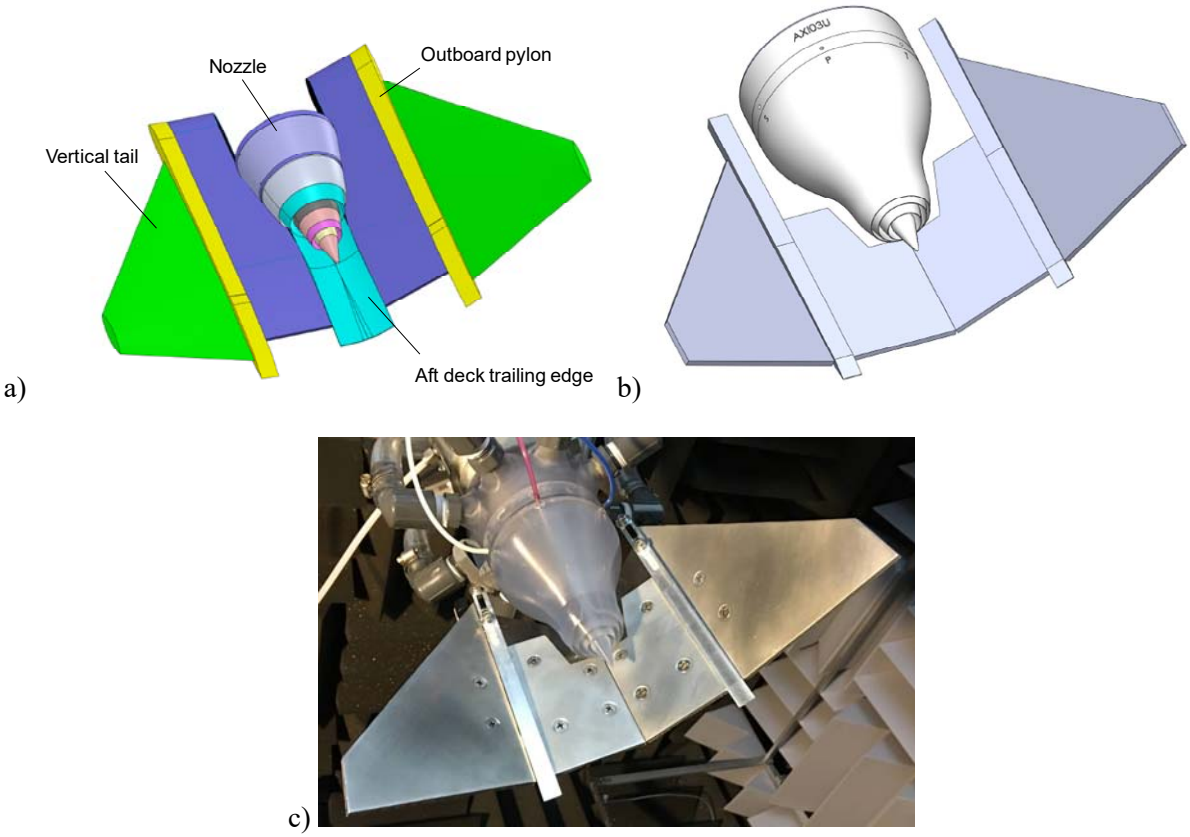

Fig. 7 Aft deck assembly. a) NASA CAD model; b) UCI CAD model; c) UCI-scale model assembled in anechoic chamber.

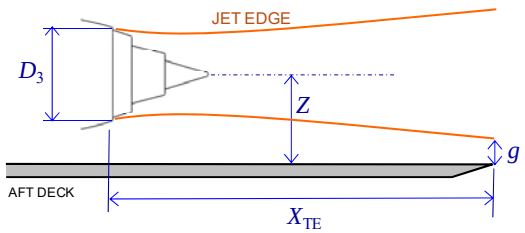

Fig. 8 Schematic detailing parameters used to define aft deck position relative to nozzle.

Table II. Nozzle and aft deck configurations

Nozzles	X_{TE}/D_3	Z
AXI03U AXI04U	2.2 (nominal)	$D_3/2$, lipline
		$g=0.1\times D_{eq}$
ECC08U ECC09U	3.7	$D_3/2$, lipline
		$g=0.1\times D_{eq}$

D. Aeroacoustic testing

Noise measurements were conducted in the UCI aeroacoustic facility shown in Fig. 9. The microphone array consists of twenty-four 1/8 in. condenser microphones (Brüel & Kjær, Model 4138) with frequency response up to 120 kHz. Twelve microphones were installed on a downward arm (ϕ=0°) and twelve were installed on a sideline arm (ϕ=60°). Figure 9(a) depicts the configuration of the downward arm; the sideline arm is practically identical. On each arm, the polar angle θ ranged approximately from 20° to 120° relative to the downstream jet axis, and the distance to the nozzle exit ranged from 0.92 m to 1.23 m. This arrangement enabled simultaneous measurement of the downward and sideline noise at all the polar angles of interest. The microphones were connected, in groups of four, to six conditioning amplifiers (Brüel & Kjær, Model 2690-A-0S4). The 24 outputs of the amplifiers were sampled simultaneously, at 250 kHz per channel, by three 8-channel multi-function data acquisition boards (National Instruments PCI-6143) installed in a Dell Precision T7400 computer with a Xeon quad-core processor. National Instruments LabVIEW software was used to acquire the signals. The temperature and humidity inside the anechoic chamber were recorded to enable computation of atmospheric absorption. The microphone signals were conditioned with a high-pass filter set at 300 Hz. Narrowband sound pressure level (SPL) spectra were computed using a 4096-point Fast Fourier Transform, yielding a frequency resolution of 61 Hz. The spectra were corrected for microphone actuator response, microphone free field response and atmospheric absorption, thus resulting in lossless spectra. For the typical testing conditions of this experiment, and for the farthest microphone location, the absorption correction was 4.5 dB at 120 kHz.

In assessing noise reduction, it is informative to convert the lab-scale frequencies to full-scale frequencies. Using the full-scale static thrust of 35,000 lb indicated in Ref. 23, the scale factor of our experiment is 45.

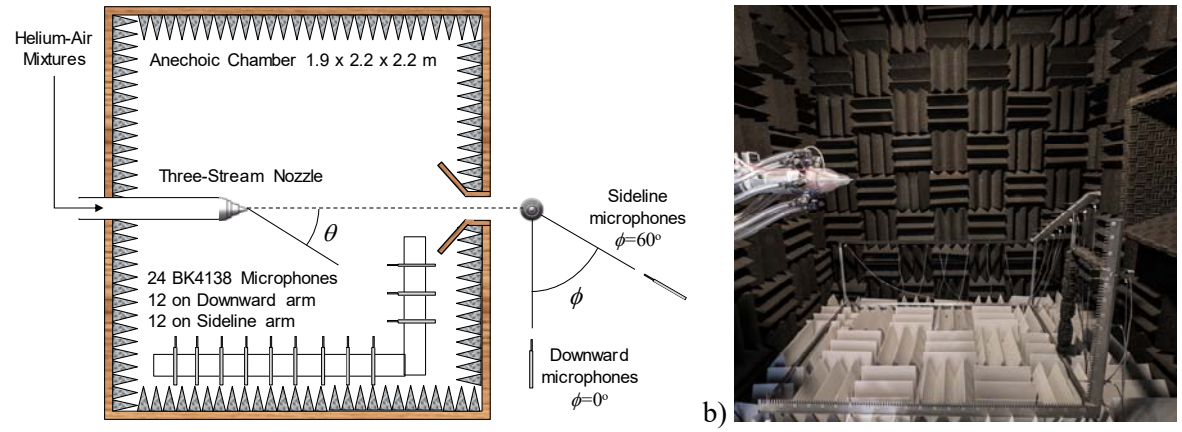

Fig. 9 UC Irvine aeroacoustics facility. a) Experimental setup; b) isolated three-stream nozzle in anechoic chamber.

III. Results

A. Effect of enlarged plug

Figure 10 compares the SPL spectra of the axisymmetric, nominal plug size nozzle, AXI03U, with the axisymmetric, enlarged-plug nozzle, AXI04U. The enlarged plug configuration is quieter by about 5 dB at high frequencies for $30° < \theta < 70°$, and most noticeably near θ=45°. Figures 11 and 12 assess the change in effectiveness of asymmetric nozzle concepts with the increased plug size. AXI03U and ECC08U are the axisymmetric and asymmetric, nominal plug size nozzles, respectively, that are selected for comparison. AXI04U and ECC09U are the axisymmetric and asymmetric enlarged plug variants of AXI03U and ECC08U, respectively.

Figure 11 compares the SPL spectra of these nozzle pairs in the downward azimuthal direction. At low polar angles, the asymmetric nozzle with the enlarged plug provides greater noise reduction at mid frequencies than its nominal-plug counterpart. As the polar angle increases, the change in spectra between the two plug sizes is nearly identical. At polar angles near 20°, the asymmetric nozzle with the enlarged plug reduces the SPL by up to 18 dB, while the asymmetric nozzle with the nominal plug reduces the SPL by up to 15 dB. The asymmetric nozzles cause a small increase in SPL at large polar angles.

Figure 12 provides similar comparisons as Fig. 11 but at the sideline azimuthal angle. There, nozzle ECC08U provides no significant noise reduction, and nozzle ECC09U offers a small reduction at low polar angles. Thus, the enlarged plug enhances the ability to reduce sideline noise, but to a limited extent.

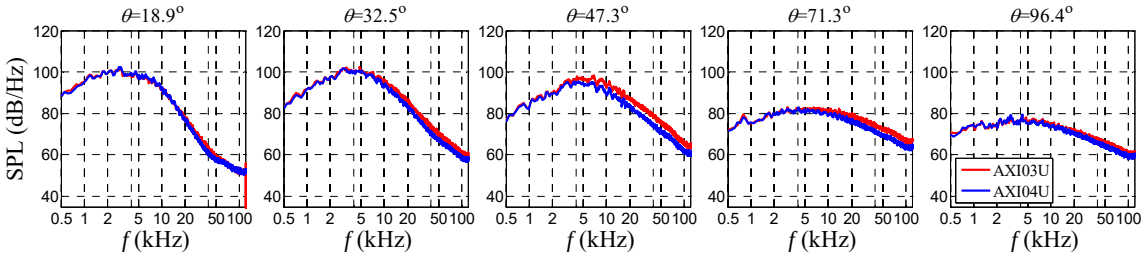

Fig. 10 SPL spectra for nozzles **AXI03U** (nominal plug) and **AXI04U** (enlarged plug).

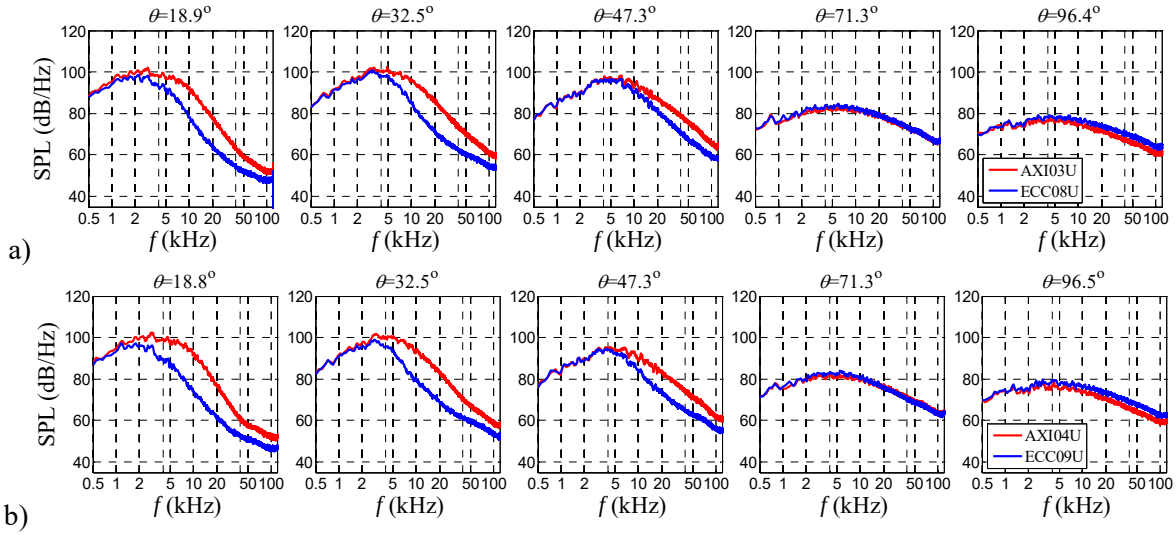

Fig. 11 SPL spectra in the downward azimuthal direction. a) Nominal-plug nozzles **AXI03U** and **ECC08U**; b) enlarged-plug nozzles **AXI04U** and **ECC09U**.

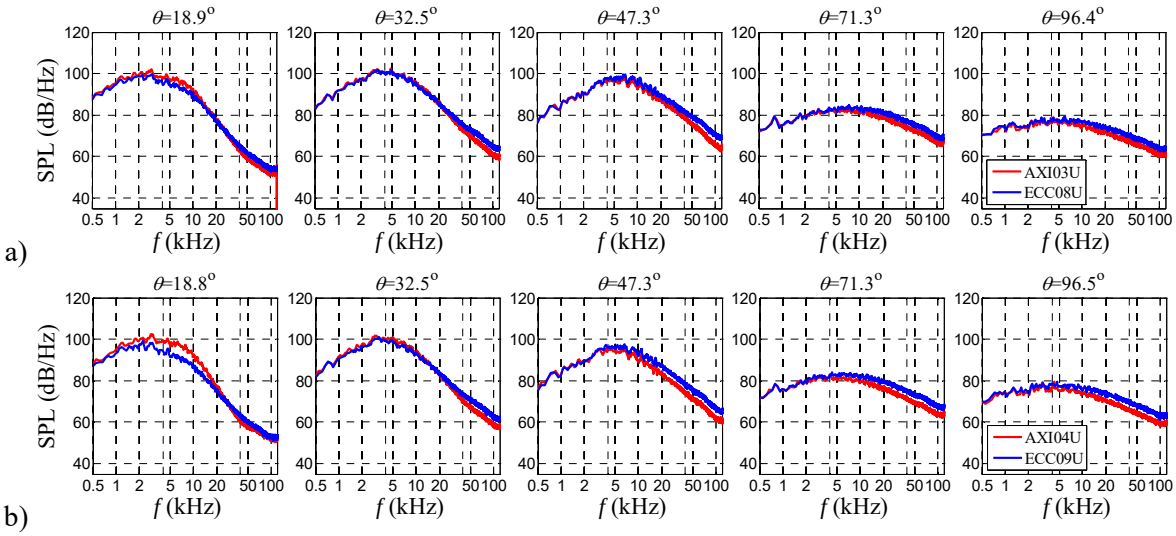

Fig. 12 SPL spectra in the sideline azimuthal direction. a) Nominal-plug nozzles **AXI03U** and **ECC08U**; b) enlarged-plug nozzles **AXI04U** and **ECC09U**.

B. Nozzles with dual asymmetry

Nozzles ECC08U and ECC09U demonstrated the capability of the tertiary stream asymmetry to reduce mixing noise (Fig. 11). The results motivated design concepts which use the secondary stream as an additional parameter space to further enhance nozzle asymmetry. All nozzles discussed in this section feature the enlarged plug. Figure 13 plots the SPL spectra for the axisymmetric nozzle AXI04U, and asymmetric nozzles ECC12U and ECC13U. Nozzle ECC12U features exit annuli asymmetry for both secondary and tertiary ducts (Fig. 5(e)), while nozzle ECC13U combines tertiary annulus asymmetry with a pair of vanes in the secondary duct (Fig. 5(f)). Comparing with Figs. 11(b) and 12(b), we note that the added asymmetry of the secondary duct improves moderately downward noise reduction and, importantly, yields significant reduction in the sideline SPL. Nozzle ECC12U provides about 2 dB stronger peak noise reduction than ECC13U in the downward direction, and 4 dB in the sideline directions, for $\theta < 49^{o}$. Figure 14 compares the SPL spectra of nozzles ECC09U and ECC12U. These nozzles were selected to isolate changes in acoustics by the addition of asymmetry to the secondary stream. Figure 14(a) indicates a 3 dB reduction in peak noise over a narrow range of polar angles, $33^{o} < \theta < 47^{o}$, in the downward direction. Nozzle ECC12U is about 6 dB quieter than ECC09U in the sideline direction, for the same range of θ.

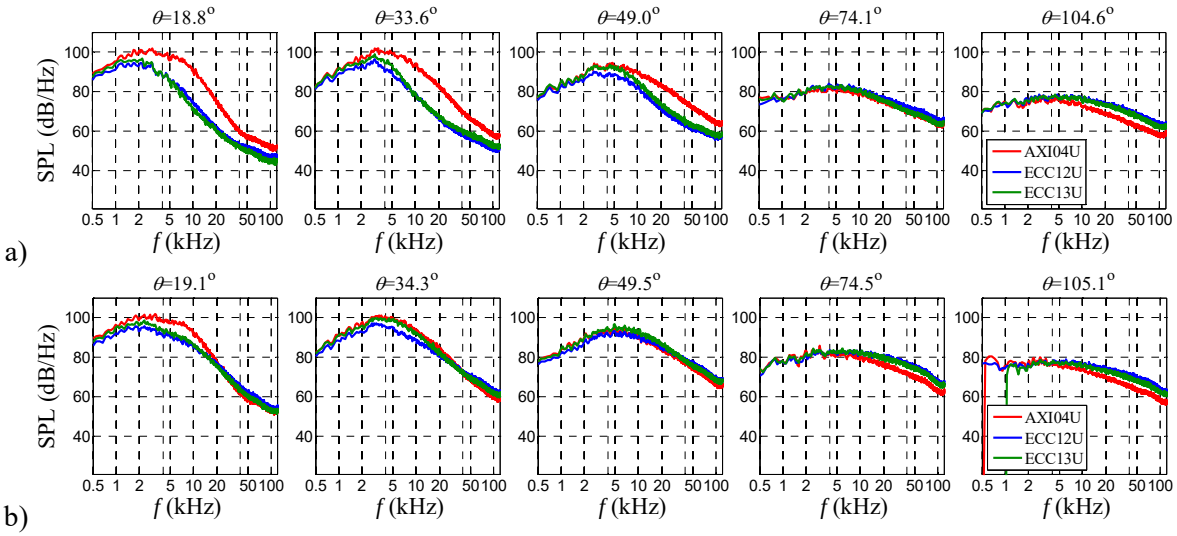

Fig. 13 SPL spectra for axisymmetric nozzle **AXI04U**, and asymmetric nozzles **ECC12U** and **ECC13U**. Measurements along a) downward, and b) sideline azimuthal directions.

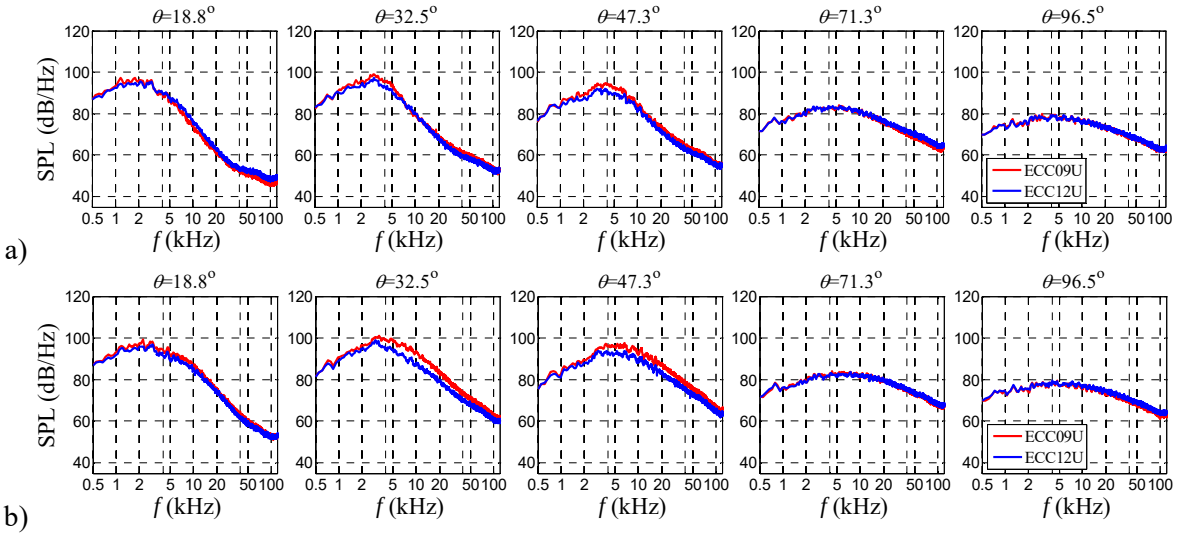

Fig. 14 SPL spectra for asymmetric nozzles **ECC09U** and **ECC12U**. Measurements along a) downward, and b) sideline direction.

C. Aft deck

Figure 15 compares the SPL spectra of the isolated and installed configurations of nozzle AXI03U, with the aft deck positioned radially at the tertiary lipline position (Z=lipline). The installed configurations are compared at two aft deck lengths: the nominal length, X_{TE}/D_3 = 2.2, and the elongated length, X_{TE}/D_3 = 3.7. The nominal aft deck produces negligible changes to the acoustics. At larger polar angles, the elongated deck amplifies low-frequency SPL by about 3 dB. Similar observations were reported in jet-surface interaction acoustic tests conducted at NASA GRC[25,26].

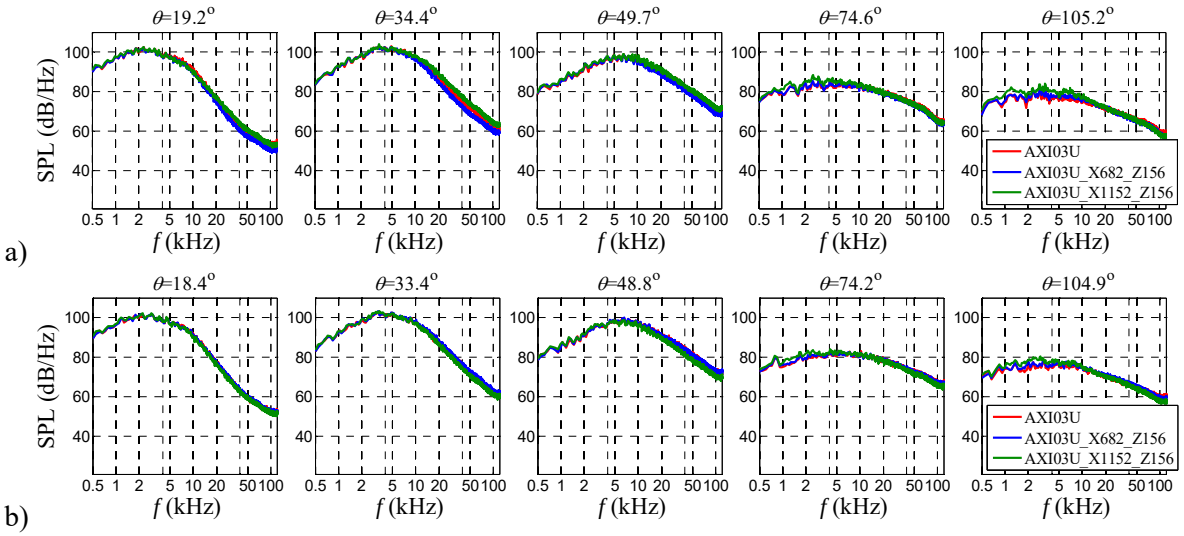

Fig. 15 SPL spectra of nozzle AXI03U in **isolated** and installed configurations with aft deck at Z = lipline, $X_{TE}/D_3 = 2.2$, and $X_{TE}/D_3 = 3.7$. Measurements along a) downward, and b) sideline directions.

Figure 16 compares the SPL spectra of the isolated and installed configurations of asymmetric nozzle ECC08U. The installed configurations compared are the nominal and elongated aft deck lengths, positioned at Z=lipline. Similar to the axisymmetric case, the nominal-length aft deck produces very little change to the acoustics of the isolated nozzle. Figure 16(a) indicates an appreciable broadband increase in the SPL spectra for $\theta < 50^o$ with the elongated deck installed. For the same polar angles, the sideline results plotted in Fig. 16(b) indicate a slight decrease in SPL. The downward amplification and sideline noise suppression are explained as follows. The downward plume asymmetry induced by the eccentric design is altered with the elongated aft deck at the lipline position. The thickened low-speed flow is likely diverted laterally along the deck, compromising its ability to reduce noise. As a result, downward noise suppression is not as effective as for the isolated nozzle (Fig. 16(a)). The slight benefit in sideline noise with the elongated deck could be the result of the lateral deflection of the low-speed flow, combined with the physical shielding by the verticals. Similar to the axisymmetric case, jet-surface interaction amplifies the low-frequency noise at polar angles $\theta > 70^o$ for the elongated deck, while a slight reduction at high frequencies is observed due to shielding.

Figure 17 plots the changes in SPL spectra for nozzle ECC08U due to varying the aft deck radial position, Z. Only results for the elongated deck length are presented; the spectra for the nominal deck length, displaced radially from the tertiary lipline, are nearly identical to those of the isolated jet. When the edge of the jet is not contacting the aft deck, nozzle ECC08U retains downward noise reduction capability similar to that of the isolated configuration. Low-frequency jet-surface interaction noise at larger polar angles is still present, even with the estimated edge of the jet above the aft deck trailing edge (Fig. 17).

Figure 18 compares the SPL spectra of the isolated and installed configurations of nozzle AXI04U. The installed configurations include the nominal and elongated aft deck lengths, positioned at Z=lipline. Compared to the nominal plug size (Fig. 16), very high frequency noise from the enlarged plug nozzle is shielded at small polar angles. The effect of the aft deck radial position on the acoustics of nozzle ECC09U is shown in Fig. 19. Similar to nozzle ECC08U, downward noise reduction is compromised with the aft deck installed at the tertiary lipline position. Displacing the elongated deck farther radially preserves the same downward reduction capability as the isolated nozzle for $\theta < 50^o$. Excess noise at large polar angles is still notable at low frequencies, with a slight improvement in high-frequency shielding over the nominal-plug configuration (Fig. 17).

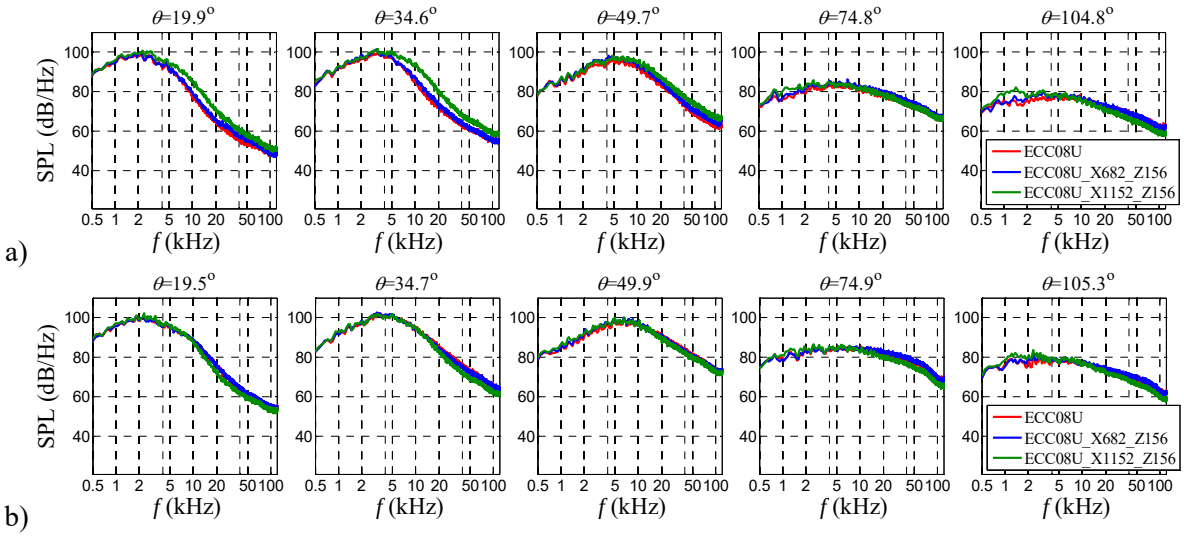

Fig. 16 SPL spectra of nozzle ECC08U in **isolated** and installed configurations with aft deck at Z = lipline, X_{TE}/D_3 = **2.2**, and X_{TE}/D_3 = **3.7**. Measurements along a) downward, and b) sideline directions.

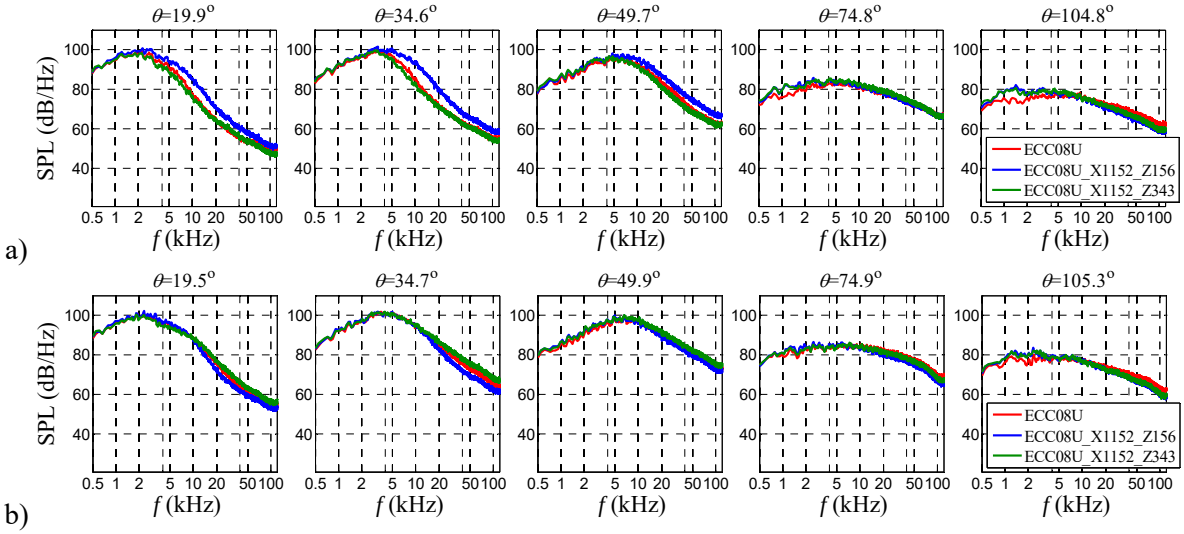

Fig. 17 SPL spectra of nozzle ECC08U in **isolated** and installed configurations with aft deck at X_{TE}/D_3 = 3.7, Z = **lipline** and $g = 0.1 \times D_{eq}$. Measurements along a) downward, and b) sideline directions.

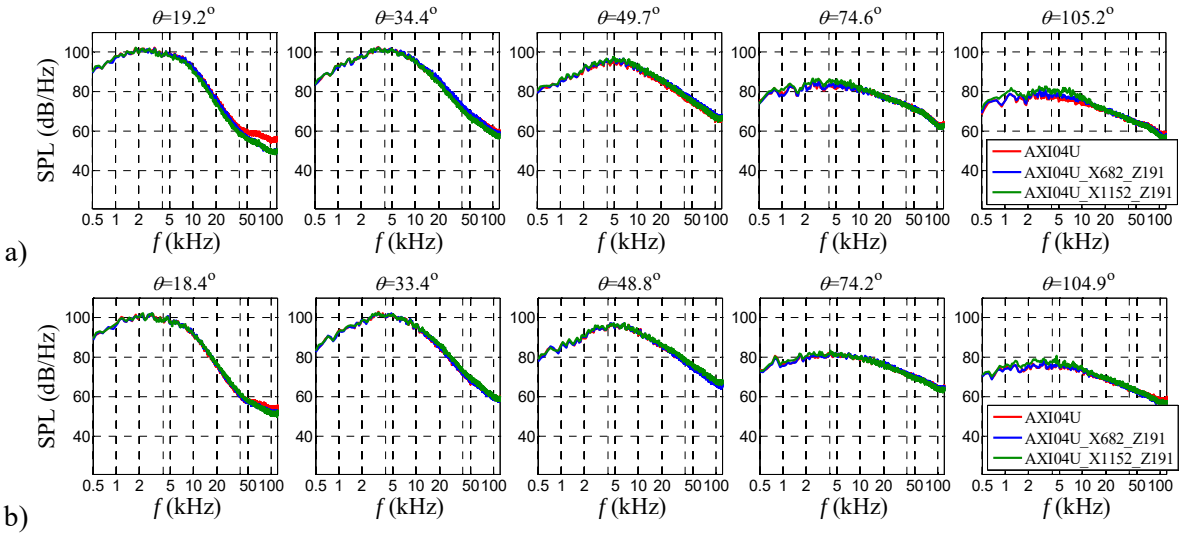

Fig. 18 SPL spectra of nozzle AXI04U in **isolated** and installed configurations with aft deck at Z = lipline, X_{TE}/D_3 **= 2.2**, and X_{TE}/D_3 **= 3.7**. Measurements along a) downward, and b) sideline directions.

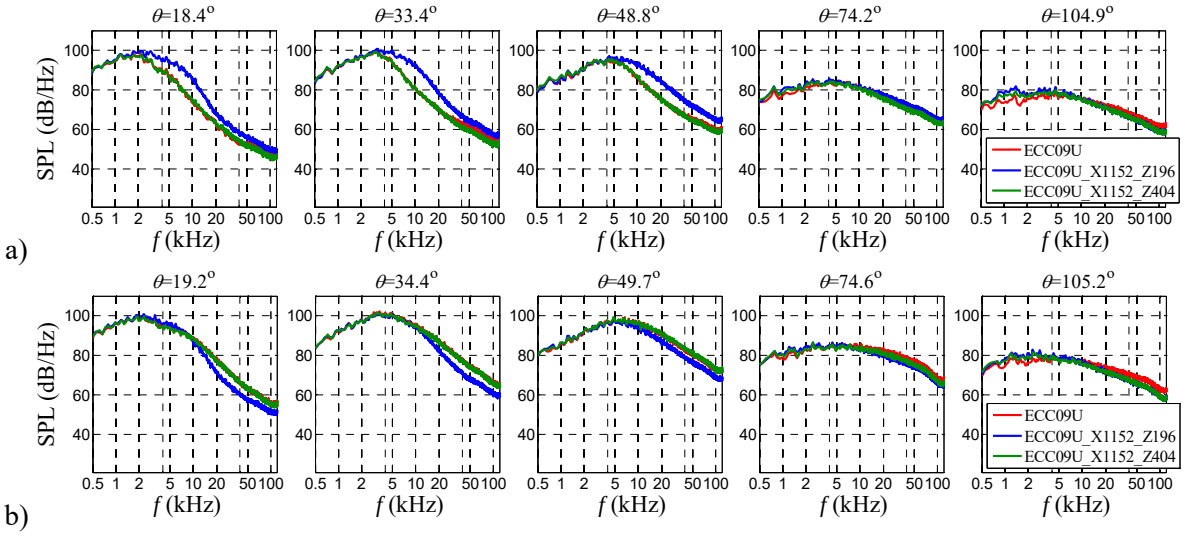

Fig. 19 SPL spectra of nozzle AXI04U in **isolated** and installed configurations with aft deck at X_{TE}/D_3 = 3.7**, Z = lipline** and g **= 0.1×**D_{eq}. Measurements along a) downward, and b) sideline directions.

The installed test results indicate that the aft deck with nominal length does not provide any significant noise shielding. Jet-surface interaction noise increases low-frequency noise for θ>75°. The downward noise reduction from asymmetric nozzle configurations is compromised when the elongated aft deck is installed at the tertiary lipline position. The elongated deck provides marginal high-frequency shielding for asymmetric nozzles ECC08U and ECC09U at θ>75°. Retaining the noise reduction capability of asymmetric nozzles with a long aft deck will require a non-scrubbing installation or contouring of the aft deck such that the flow asymmetry is preserved. It is in fact possible that innovative designs of the aft deck, carefully integrated with the nozzle, will enhance the ability of asymmetric nozzles to reduce noise.

The aft deck lengths tested in this study extended 2.2 and 3.7 tertiary exit diameters downstream of the tertiary exit plane. Noise source maps for externally-plugged, externally-mixed, dual-stream nozzles indicate that the jet noise source is strongly localized slightly over 4 fan diameters downstream of the exit

plane[27]. It is likely that the aft deck lengths in this study are not sufficiently shielding the noise source region. Further work to improve jet noise shielding would require devices, such as chevrons, to compact the noise source region, or extending the aft deck trailing edge even farther downstream.

IV. Conclusions

We present advances in three-stream nozzle design concepts with potential to reduce takeoff noise from future supersonic aircraft. The point of departure from previous designs[22] involved increasing the plug size, examining combined asymmetry in secondary and tertiary flows, and investigating installation effects with an aft deck. The enlarged plug is a design modification aimed to maintain low-sonic-boom compatibility by mitigating the adverse effects of abrupt nacelle diameter changes associated with the short-cowl designs of Ref. 22. The axisymmetric nozzle with enlarged plug is inherently quieter, by as much as 5 dB, than its nominal-plug counterpart. The enlarged plug also adds incrementally to the already large noise reduction (as much as 15 dB) enabled by configurations featuring asymmetric tertiary ducts, improving it by about 3 dB at low polar angles.

Asymmetry in the secondary flow involved installing a pair of deflector vanes inside the secondary duct or reshaping eccentrically the secondary annulus. The case with eccentric secondary annulus was more effective in reducing noise. Compared with the nozzles with asymmetry only in the tertiary duct, the combined secondary-tertiary asymmetry reduced noise by as much as 3 dB in the downward direction and 6 dB in the sideline direction, at polar angles near the direction of peak emission. If we combine the effect of the enlarged plug with the optimal eccentric configuration, the noise reduction from the baseline is 15 dB downward and 6 dB sideline at polar angles near the direction of peak emission and full-scale frequency around 300 Hz.

In the study of installation effects, the aft deck geometry was modeled from the Lockheed Martin low-boom concept vehicle[23]. The aft deck trailing edge position was varied radially from a lipline (scrubbing) position to a position where no significant scrubbing was expected. The trailing edge to nozzle axial distance was varied from the nominal value to 1.7 times the nominal value. The nominal-deck length, at either radial position, caused minimal changes to the acoustics. The elongated deck provided a small amount of shielding at large polar angles and high frequency, accompanied by modest excess noise at low frequency. Importantly, the elongated deck at the scrubbing position caused a marked deterioration in the noise reduction of the asymmetric nozzles.

Acknowledgment

We acknowledge the support by NASA Cooperative Agreement NNX14AR98A, monitored by Dr. James Bridges. We thank Dr. Juntao Xiong for the RANS data of the flow field.

References

1. Welge, R. H., Nelson, C., and Bonet, J., "Supersonic Vehicle Systems for the 2020 to 2035 Timeframe," AIAA Paper 2010-4930, June 2010.
2. Dickson, N., "ICAO Noise Standards," *ICAO Symposium on Aviation and Climate Change, "Destination Green,"* May 2013.
3. Huff, D. L., Henderson, B. S., Berton, J. J., and Seidel, J. A., "Perceived Noise Analysis for Offset Jets Applied to Commercial Supersonic Aircraft," AIAA Paper 2016-1635, Jan. 2016.
4. Tam, C. K. W., "Supersonic jet noise," *Annual Review of Fluid Mechanics*, Vol. 27, 1995, pp. 17-43.
5. McLaughlin, D. K., Morrison, G. L., and Troutt, T. R., "Experiments on the Instability Waves in a Supersonic Jet and their Acoustic Radiation," *Journal of Fluid Mechanics*, Vol. 69, No. 1, 1975, pp. 73-95.
6. Laufer, J., Schliner, R. and Kaplan, R. E., "Experiments on Supersonic Jet Noise," *AIAA Journal*. Vol. 14, No. 4, 1976, pp. 489-497.
7. Papamoschou, D., "Mach Wave Elimination in Supersonic Jets," *AIAA Journal*. Vol. 35, No. 10, 1997, pp. 1604-1611.

8. Panda, J. and Seasholtz, R. G., "Experimental Investigation of Density Fluctuations in High-Speed Jets and Correlation with Generated Noise," *Journal of Fluid Mechanics*, Vol. 450, 2002, pp. 97-130.

9. Tam, C. K. W., Viswanathan, K., Ahuja, K. K., and Panda, J., "The Sources of Jet Noise: Experimental Evidence," *Journal of Fluid Mechanics*, Vol. 615, Nov. 2008, pp. 253-292.

10. Tam, C. K. W., "Mach Wave Radiation from High-Speed Jets," *AIAA Journal*, Vol. 47, No. 10, 2009, pp. 2440-2448.

11. Papamoschou, D. and Debiasi, M., "Directional Suppression of Noise from a High-Speed Jet," *AIAA Journal*, Vol. 39, No. 3, 2001, pp. 380-387.

12. Papamoschou, D., "New Method for Jet Noise Suppression in Turbofan Engines," *AIAA Journal*, Vol. 42, No. 11, 2004, pp. 2245-2253.

13. Brown, C. A., Bridges, J. E., and Henderson, B., "Offset Stream Technology Test—Summary of Results," AIAA Paper 2007-3664, Jan. 2007.

14. Papamoschou, D., Debiasi, M., "Noise Measurements in Supersonic Jets Treated with the Mach wave Elimination Method," *AIAA Journal*. Vol. 37, No. 2, 1999, pp. 154-160.

15. Zaman, K. B. M. Q., "Noise- and Flow-Field of Jets from an Eccentric Coannular Nozzle," AIAA Paper. 2004-0005, Jan. 2004.

16. Dippold, V., Foster, L., Wiese, M. "Computational Analyses of Offset-Stream Nozzles for Noise Reduction," *Journal of Propulsion and Power*, Vol. 25, No. 1, Jan.-Feb. 2009.

17. DeBonis, J.R., "RANS Analyses of Turbofan Nozzles with Internal Wedge Deflectors for Noise Reduction," *Journal of Fluids Engineering*, Vol. 131, April 2009, Article 041104.

18. Henderson, B. S., "Aeroacoustics of Three-Stream Jets," AIAA Paper 2012-2159, June 2012.

19. Henderson, B. S., Lieb, S. J., and Wernet, M., "Measurements and Predictions of the Noise from Three-Stream Jets," AIAA Paper 2015-3120, Jan. 2015.

20. Henderson, B. S., and Wernet, M. P., "Characterization of Three-Stream Jet Flow Fields," NASA/TM-2016-219098, July 2016.

21. Papamoschou, D., Johnson, A.D., and Phong, V., "Aeroacoustics of Three-Stream High-Speed Jets from Coaxial and Asymmetric Nozzles," *Journal of Propulsion and Power*, Vol. 30, No. 4, 2014, pp. 1055-1069.

22. Papamoschou, D., Phong, V., Xiong, J., and Liu, F., "Quiet Nozzle Concepts for Three-Stream Jets," AIAA Paper-2016-0523, Jan. 2016.

23. Morgenstern, J., Buonanmo, M., Yao, J., Muruappan, M., Paliath, U., Cheung, L., Malcevic, I., Martens, S., Viars, P., Tersmette, T., Lee, J., Simmons, R., Plybon, D., Alonso, J., Palacios, F., Lukaczyk, T., Carrier, G., "Advanced Concept Studies for Supersonic Commercial Transports Entering Service in the 2018-2020 Period Phase 2," NASA/CR-2015-218719, July 2015.

24. Papamoschou, D., "Acoustic Simulation of Coaxial Hot Air Jets Using Cold Helium-Air Mixture Jets," *Journal of Propulsion and Power*, Vol. 23, No. 2, 2007, pp. 375-381.

25. Head, R. W. and Fisher, M. J., "Jet/Surface Interaction Noise: Analysis of Farfield Low Frequency Augmentations of Jet Noise due to the Presence of a Solid Shield," AIAA Paper 76-502, July 1976.

26. Brown, C., "Jet-Surface Interaction Test: Far-Field Noise Results," *Proceedings of the ASME Turbo Expo 2012*, GT2012-69639, June 2011.

27. Papamoschou, D. and Mayoral, S., "Experiments on Shielding of Jet Noise by Airframe Surfaces," AIAA-2009-3326, May 2009.